Iberfault 2022

IV Reunión Ibérica
sobre Fallas Activas y Paleosismología

TERUEL · 7 al 10 de septiembre de 2022

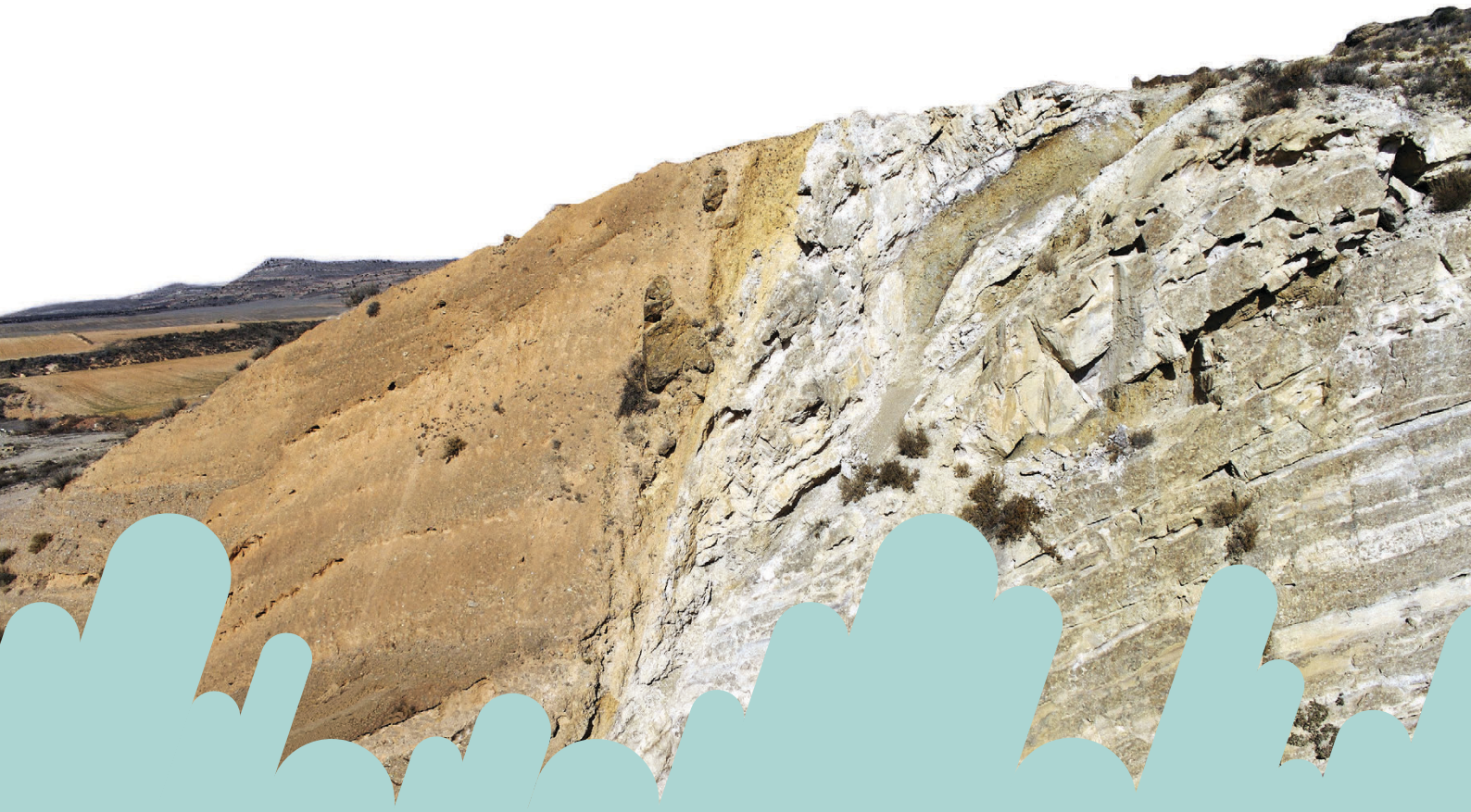

VOLUMEN DE RESÚMENES

IBERFAULT 2022

IV Reunión Ibérica sobre Fallas Activas y Paleosismología

TERUEL · 7 al 10 de septiembre de 2022

VOLUMEN DE RESÚMENES

Editores:

Iván Martín, Carlos L. Liesa, Pedro Alfaro, Carolina Canora, Lope Ezquerro, Jesús Galindo, José J. Martínez, Alba Peiro, Óscar Pueyo, José L. Simón

Los trabajos contenidos en el presente volumen deberán citarse como en el siguiente ejemplo:

García-Mayordomo, J. y Martín-Banda, R. (2022). Prospectiva de zonas de interés para el desarrollo futuro de estudios de actividad tectónica reciente en España. *Resúmenes IV Reunión Ibérica sobre Fallas Activas y Paleosismología*, Teruel, Universidad de Zaragoza, pp. 177-180.

D.L.: Z 1059-2022

ISBN: 978-84-18321-58-0

Servicio de Publicaciones
Universidad Zaragoza

© Los autores

Editores:
Iván Martín, Carlos L. Liesa, Pedro Alfaro, Carolina Canora, Lope Ezquerro, Jesús Galindo, José J. Martínez, Alba Peiro, Óscar Pueyo, José L. Simón

Diseño: Alba Peiro

Editado por:
Departamento de Ciencias de la Tierra, Universidad de Zaragoza.

Fotografía de portada: Falla de Concud en Los Baños, Teruel. Autora: Paloma Lafuente.

SEISMOGENIC DEPTH IN IBERIA

Álvaro González[1], Ángela María Gómez-García[2]

[1] CRM Centre de Recerca Matemàtica. Campus UAB Edifici C, 08193 Bellaterra, Barcelona, Spain. alvaro@geonaut.eu
[2] GFZ German Research Centre for Geosciences, 14473 Telegrafenberg, Potsdam, Germany. angela@gfz-postdam.de

Abstract: We present the first, preliminary maps of the lower seismogenic depth for the whole Iberian Peninsula and surroundings. This depth is calculated as the 90% percentile (d_{90}) of the hypocentral depth distribution of earthquakes immediately surrounding each site of the map, considering only those events with the most reliable locations. Two versions of this map are shown: either considering earthquakes at all depths, or restricting the analysis to crustal seismicity. The resulting values of d_{90} can be used as a proxy of the brittle-ductile transition, as well as in seismic hazard assessment in order to define the lower depth boundary of seismogenic sources. For example, as the effective lower boundary of crustal faults (considering the map calculated with crustal earthquakes), especially if fault geometries are not constrained by other means. Regional variations of d_{90} are emphasized, ranging from values as low as ~4 km for seismicity associated to the Castor project to 375 km below Granada, and may be largely interpreted considering each local tectonic setting. Such d_{90} maps provide also observational constraints for future thermal and rheological modelling of the Iberian lithosphere.

Key words: Iberian Peninsula, hypocentral depth, statistical seismology, seismic hazard assessment.

Introduction

Earthquake ruptures nucleate in the seismogenic layer, where the rheology of the rocks allows stick-slip dynamics with the release of short-period seismic waves during sudden slip (e.g. Scholz, 2019). The relevant lower limit of seismogenic sources for the purpose of modelling in seismic hazard assessment is the lower boundary of this layer, which corresponds to the brittle-ductile transition. This transition is usually deduced as the lower depth limit of the observed distribution of seismicity. From the recorded earthquakes alone, it is not possible to define a strict limit (such as 100% of them nucleate above that limit and 0% of them nucleate below), since there is always some probability that an earthquake deeper than those observed could eventually occur. For this reason, a percentile of earthquake depths is usually regarded as a statistically meaningful lower boundary of the seismogenic zone. The most commonly used limit is the 90% percentile (Sibson, 1982), denoted d_{90}, defined such as 90% of earthquakes in a region are shallower than d_{90}.

It may also be useful to consider a crustal seismogenic depth, calculated only with earthquakes not deeper than the Mohorovicic discontinuity (Wu *et al*., 2017). This allows determining the maximum seismogenic depth of crustal faults, separately from the global deeper seismogenic depth, which also involves earthquakes generated by sub-crustal structures. Considering explicitly that discontinuity (as Wu *et al*., 2017) is not common when calculating seismogenic depths. No lower hypocentral depth threshold is typically used (e.g. Zuza and Cao, 2020) or some maximum threshold is chosen arbitrarily.

This work presents preliminary maps of seismogenic depth for the whole Iberia and surrounding regions, either considering all the seismicity (regardless of its depth) or crustal earthquakes only. Previously, the seismogenic depth had been mapped in detail only for NW Iberia (Llana-Fúnez and López-Fernández, 2015), albeit interpolating the depth of the deepest earthquakes in the region, instead of considering depth percentiles.

Data used

Earthquake catalogue

The catalogue of the National Geographic Institute of Spain (IGN, 2022) is used (Fig. 1), whose quality was analysed by González (2017, 2018). Despite the catalogue covers the seismicity recorded since the historical era (before the XX century), and a telemetred network was operational since 1985, the precision of the reported hypocentral depths is particularly reliable since November 1997, when the IGN location software was updated; since this date, hypocentral depth uncertainties were reported with the same criterion (see González, 2017, 2018 for details). In the Iberian Peninsula and surroundings, the catalogue is complete down to a completeness magnitude M_c~2.8 or better during November 1997-February 2002, and down to M_c~2.0 or better since March 2002 (González, 2017, 2018). Therefore, we used these periods and magnitude thresholds for our analysis, including events recorded up to April 2022.

Hypocentral depth is the most difficult location parameter to determine. For a substantial fraction of events in the catalogue, it is reported as 0 km, or could not be calculated independently from the available phase pickings and is flagged as fixed (González, 2017). In either case, such events are removed from the present analysis, as they would artificially distort the actual depth distribution. For events with non-fixed depth (that is, calculated from the available data), depth errors (reported as 90% uncertainty intervals) are typically ~5 km within the Iberian Peninsula but increase rapidly offshore, far from the recording network (González, 2017, 2018). Hypocentres with effectively unconstrained depths (reported 90% error larger than 30 km) were also excluded from our analysis (Fig. 1).

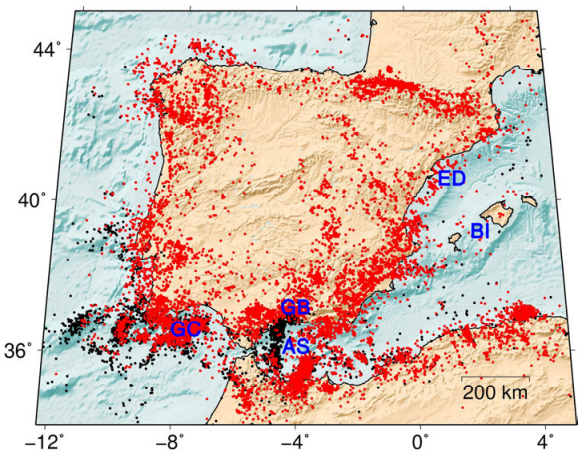

Fig. 1.- Earthquakes used for calculating the seismogenic depth. Black: Sub-crustal; Red: Crustal. Blue labels: Locations mentioned in the main text: AS: Alboran Sea; BI: Balearic Islands; ED: Ebro Delta; GB: Granada Basin; GC: Gulf of Cádiz.

Geoid height

Hypocentral depths in the IGN catalogue are referred to the WGS84 ellipsoid. In order to consider the actual depth below sea level, they were referred to the EGM2008-5 geoid model (Pavlis *et al*., 2012).

Bathymetry

The location procedures used by IGN (and most seismological agencies) consider an Earth model with horizontal layers with different seismic wave velocities. This disregards the actual topography or bathymetry, and may yield hypocentral depths located in ocean water. When regarding crustal seismicity, we discarded such earthquakes, considering the GEBCO bathymetry model as reference (GEBCO Bathymetric Compilation Group, 2020).

Moho depth

The depth to the base of the crust (Mohorovicic discontinuity, or Moho for short) was taken as the average value mapped in the detail in the PRISM3D model (Arrocau *et al*., 2021), the most recent one published for the Iberian region.

Method of percentile calculation

The 90% depth percentile (d_{90}) was calculated using the median-unbiased estimator of Hyndman and Fan (1996) at each node of a latitude-longitude grid with a spacing of 0.1°. We use the 20 closest earthquakes to each node as the sample for calculating the corresponding d_{90}, provided that they are at a maximum distance of 100 km from the node (to avoid regions where the spatial density of epicentres is too low to obtain reliable results), and provide d_{90} as the average value obtained from 10000 bootstrap samples (Efron, 1979).

Firstly, we use all earthquakes in the catalogue which satisfy the quality criteria mentioned in the section above. For a second analysis, we consider only the subset of those earthquakes which are located within the crust (below the topography or seafloor, and not deeper than the Moho).

Seismogenic depth

The resulting maps of d_{90} are shown in Figures 2A (calculated using all earthquakes) and 2B (calculated using crustal earthquakes only). The results of Figure 2A can be summarized as follows. Most values below the Iberian Peninsula, where seismicity is mainly generated by crustal faults (e.g. García-Mayordomo *et al*., 2012) are located within the continental crust (typically d_{90}<25 km). The western half of the peninsula, approximately where the crystalline basement of the Paleozoic Iberian Massif crops out, shows typically higher d_{90} than the eastern part. The spot with lowest d_{90} values in the maps (~4 km) is associated to the seismicity triggered by the Castor project (e.g. Cesca *et al*., 2021 and references therein), offshore the Mediterranean coast close to the Ebro Delta, evidencing that it was shallower than the typical, natural, seismicity. Large d_{90} values (> 60 km, and even >100 km) are reached offshore, in the Gulf of Cadiz (characterized by cold, ancient oceanic lithosphere, where part of the seismicity occurs in the mantle, e.g. Custódio *et al*., 2015) and in the Alboran Sea (due to its intermediate-depth seismicity. e.g. López-Sánchez *et al*., 2002).

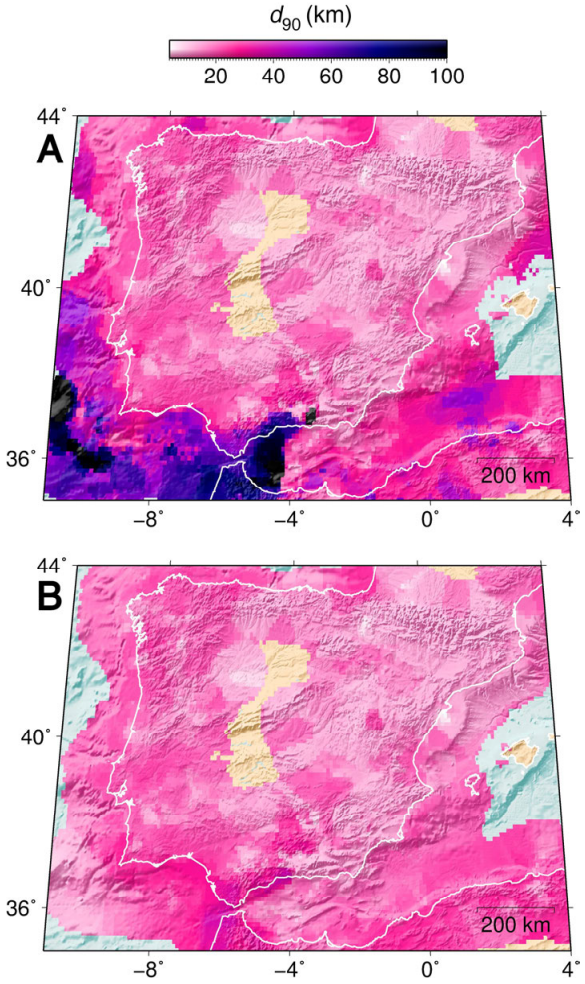

Fig. 2.- Map of the seismogenic depth (d_{90}, the 90% hypocentral depth percentile) in the Iberian Region. A (top): Calculated considering earthquakes regardless of their depth. The observed range is from 4 to 375 km, albeit the colour scale is truncated at 100 km for clarity. B (bottom): Calculated using crustal earthquakes only. For comparison, the same colour scale as in (A) is used. The observed range is from 4 to 38 km. In regions with a too low spatial density of earthquakes, d_{90} was not calculated and they appear without results (e.g. centre of the Iberian Peninsula).

In specific locations in Morocco, Algeria and offshore between the Balearic Islands and the African coast, values reaching 50 km are observed, albeit in those areas the earthquake catalogue is less complete than in or near the Iberian Peninsula (González, 2017, 2018), so these d_{90} values would need to be taken with caution. The largest d_{90} values (~375 km) are observed where deep earthquakes have occurred near the Granada Basin (e.g. Bezada and Humpfreys, 2012, and references therein). This is an example of the limits of the usefulness of such unconstrained d_{90} values for seismic hazard assessment, since the hazard at this location is controlled by shallower seismic sources (e.g. Peláez Montilla *et al*., 2003).

Restricting the analysis to crustal seismicity (Fig. 2B), logically the maximum d_{90} values are equal to or smaller than in Figure 2A, reaching up to ~38 km. The most notable differences with Figure 2A are found in the shallower values observed in offshore regions, northern Africa and the Gibraltar Arc. The Moho depth (disregarding its reported uncertainties; Arrocau *et al*., 2021) provides an upper constraint to d_{90} of Figure 2B. Apart from this limitation, there is no simple, direct correlation between the Moho depth and d_{90}, as noted elsewhere (e.g. Wu *et al*., 2017). For example, the thick crust under the Pyrenees does not show large d_{90} values, while the western margin of the peninsula, with thinner crust (Arroucau *et al*., 2021), shows higher d_{90} values instead.

Conclusions

The available earthquake data (IGN, 2022) is already reliable and abundant enough to map the seismogenic depth in detail in the Iberian region and surroundings. This work presents the first, preliminary, maps of the 90% hypocentral depth percentile (d_{90}) in the whole region. This proxy to the brittle-ductile transition shows considerable variability, and may be largely interpreted as related to the diverse tectonic settings present in the region. For example, crustal faulting within the peninsula, intermediate-depth seismicity in the Alboran Arc, deep earthquakes below Granada and seismicity in the mantle below the Gulf of Cadiz.

The seismogenic depth, even if restricted to crustal earthquakes, is only poorly correlated with the Moho depth (e.g. Wu *et al*., 2017), as it also depends on the lithological, thermal and rheological characteristics of the lithosphere. For this reason, d_{90} provides a more reliable lower depth boundary of seismogenic sources than the Moho depth *per se*. Such a boundary can be applied to crustal seismogenic sources when the map is calculated using crustal earthquakes.

Finally, the d_{90} values mapped here provide observational constraints for future modelling attempts of the thermal and rheological structure under Iberia.

Acknowledgements

Á.G. is supported by the “Juan de la Cierva-Incorporación” grant IJC2020-043372-I from the Spanish State Research Agency.

References

Arroucau, P., Custódio, S., Civiero, C., Silveira, G., Dias, N., Díaz, J., Villaseñor, A., Bodin, T., 2021. PRISM3D: a 3-D reference seismic model for Iberia and adjacent areas. *Geophysical Journal International*, 225: 789-810.

Bezada M.J., Humphreys, E.D., 2012. Contrasting rupture processes during the April 11, 2010 deep-focus earthquake beneath Granada, Spain. *Earth and Planetary Science Letters* 353-354: 38-46.

Cesca, S., Stich, D., Grigoli, F., Vuan, A., López-Comino, J.A., Niemz, P., Blanch, E., Dahm, T., Ellsworth, W.L., 2021. Seismicity at the Castor gas reservoir driven by pore pressure diffusion and asperities loading. *Nature Communications*, 12: 4783.

Custódio, S., Dias, N.A., Carrilho, F., Góngora, E., Rio, I., Marreiros, C., Morais, I., Alves, P., Matias, L., 2015. Earthquakes in western Iberia: improving the understanding of lithospheric deformation in a slowly deforming region. *Geophysical Journal International*, 203: 127-145.

Efron, J., 1979. Bootstrap methods: Another look at the jackknife. *The Annals of Statistics*, 7: 1-26.

García-Mayordomo, J., Insua-Arévalo, J.M., Martínez-Díaz, J.J., Jiménez-Díaz, A., Martín-Banda, . R., Martín-Alfageme, S., Álvarez-Gómez, J.A., Rodríguez-Peces, M., Pérez-López, R., Rodríguez-Pascua, M.A., Masana, E., Perea, H., Martín-González, F., Giner-Robles, J., Nemser, E.S., Cabral J. and the QAFI Compilers Working Group, 2012. The Quaternary Faults Database of Iberia (QAFI v.2.0), *Journal of Iberian Geology*, 38: 285-302.

GEBCO Bathymetric Compilation Group, 2020. *The GEBCO_2020 Grid - A continuous terrain model of the global oceans and land*. British Oceanographic Data Centre, National Oceanography Centre, NERC, UK. DOI:dtg3

González, Á., 2017. The Spanish National Earthquake Catalogue: Evolution, precision and completeness. *Journal of Seismology*, 21: 435-471.

González, Á., 2018. El catálogo sísmico del Instituto Geográfico Nacional: una guía para el usuario. *Tercera reunión ibérica sobre fallas activas y paleosismología, Alicante (España)*, 257-260.

Hyndman, R.J., Fan, Y., 1996. Sample quantiles in statistical packages. *American Statistician*, 50: 361-365.

IGN -Instituto Geográfico Nacional- (2022). Catálogo de terremotos. DOI:10.7419/162.03.2022

Llana-Fúnez, S., López-Fernández, C., 2015. The seismogenic zone of the continental crust in Northwest Iberia and its relation to crustal structure. *Tectonics*, 34: 1751-1767.

López-Sánchez, C., Buforn, E., Cesca, S., Lozano, L., Sanz de Galdeano, C., Mattesini, M., Udías, A., Cantavella, J.V., 2002. Intermediate-depth earthquakes in southern Spain and Alboran Sea. *Tectonophysics*, 825: 229238.

Pavlis, N.K., Holmes, S.A., Kenyon, S.C., Factor, J.K., 2012. The development and evaluation of the Earth Gravitational Model 2008 (EGM2008). *Journal of Geophysical Research*, 117: B04406.

Peláez Montilla, J.A., Sanz de Galdeano, C., López Casado, C., 2003. Use of active fault data versus seismicity data in the evaluation of seismic hazard in the Granada Basin (Southern Spain). *Bulletin of the Seismological Society of America*, 93:1670-1678.

Scholz, C.H., 2019. *The Mechanics of Earthquakes and Faulting*, 3rd edition. Cambridge University Press, Cambridge, United Kingdom, 493 p.

Sibson, R.H., 1982. Fault zone models, heat flow, and the depth distribution of earthquakes in the continental crust of the United States. *Bulletin of the Seismological Society of America*, 72:151-163.

Wu, W.N., Yen, Y.T., Hsu, Y.J., Wu, Y.M., Lin, J.Y., Hsu, S.K., 2017. Spatial variation of seismogenic depths of crustal earthquakes in the Taiwan region: Implications for seismic hazard assessment. *Tectonophysics*, 708: 81-95.

Zuza, A.V., Cao, W., 2020. Seismogenic thickness of California: Implications for thermal structure and seismic hazard. *Tectonophysics*, 782-783:228426.